A Cascade Hybrid PSO Feed-Forward Neural Network Model of a Biomass Gasification Plant for Covering the Energy Demand in an AC Microgrid

Cristian Chiñas-Palacios[a,b], Carlos Vargas-Salgado[a,c]*, Jesus Aguila-Leon[a,b] and Elias Hurtado-Pérez[a,b]

[a] *Instituto Universitario de Ingeniería Energética, Universitat Politècnica de València, València, España*

[b] *Departamento de Estudios del Agua y de la Energía, Centro Universitario de Tonalá de la Universidad de Guadalajara, Tonalá, México*

[c] *Departamento de Ingeniería Eléctrica, Universitat Politècnica de València, València, España.*

*corresponding author

Abstract

Agriculture and forestry crop residues represent more than half of the world's residual biomass; these residues turn into synthesis gas (syngas) and are used for power generation. Including Syngas Gensets into hybrid renewable microgrids for electricity generation is an interesting alternative, especially for rural communities where forest and agricultural waste are abundant. However, energy demand is not constant throughout the day. The variations in the energy demand provoke changes in both gasification plant efficiency and biomass consumption. This paper presents an Artificial Neural Network (ANN) based model hybridized with a Particle Swarm Optimization (PSO) algorithm for a Biomass Gasification Plant (BGP) that allows estimating the amount of biomass needed to produce the required syngas to meet the energy demand. The proposed model is compared with two traditional models of ANNs: Feed Forward Back Propagation (FF-BP) and Cascade Forward Propagation (CF-P). ANNs are trained in MATLAB software using a set of historical real data from a BGP located in the Distributed Energy Resources Laboratory of the Universitat Politècnica de València in Spain. The model performance is validated using the Mean Squared Error (MSE) and linear regression analysis. The results show that the proposed model performs 23.2%

better in terms of MSE than de other models. The tunning parameters of the optimal PSO algorithm for this application were found. Finally, the model was validated to predict the necessary biomass and syngas to cover the energy demand.

Keywords: Artificial Neural Network Model; Particle Swarm Optimization; AC Microgrid; Syngas Genset.

Nomenclature

ANN	Artificial Neural Network
BGP	Biomass Gasification Plant
BGP	Biomass Gasification Plant plus Genset
BP	Back Propagation
c_1	PSO particle personal acceleration coefficient
c_2	PSO particle social acceleration coefficient
CF-P	Cascade Forward Propagation
CH_4[%]	Methane Percentage
CO_2	Carbon Dioxide
CO_2[%]	Carbon Dioxide Percentage
CONACYT	Consejo Nacional de Ciencia y Tecnología
E	Error
EBPGS	Energy Backup Power Generation Systems
EMS	Energy Management System
ESS	Energy Storage Systems
F	Frequency
F_{act_i}	ANN Activation Function
FF-BP	Feed Forward Back Propagation

FIS	Fuzzy Inference System
f_{min}	Objective Function to be minimized
F_{pro_n}	ANN Propagation Function
GA	Genetic Algorithm
Genset	Internal combustion engine plus synchronous generator
$H_2[\%]$	Hydrogen Percentage
HRES	Hybrid Renewable Energy Systems
ICE	Internal Combustion Engine
LabDER-UPV	Distributed Energy Resources Laboratory of the Universitat Politècnica de València
LHV	Lower Heating Value
M	Biomass flow
MG	Microgrids
MLP	Multilayer-Perceptron
MSE	Mean Squared Error
N	Number of samples
N_2 [%]	Nitrogen Percentage
o_{i_j}	ANN weighted output
$o_{predicted}$	Predicted Output
o_{target}	Target Output
P	Active Power
PF	Power Factor
PSO	Particle Swarm Optimization
PV	Photovoltaic

$Q_{air_{gasifier}}$	Airflow to the reactor
$Q_{air_{ICE}}$	Airflow to the ICE
Q_{syngas}	Syngas flow
RBF	Radial Basis Function
RES	Renewable Energy Source
T_{env}	Environmental Temperature
T_1	Temperature of the reactor
TEG	Hybrid Thermoelectric Generator
v_n	PSO particle velocity function
$w_{i_1,j}$	Neuron weight
WTG	Wind Turbine Generator
X_i	Optimization variables vector
$Y_{predicted}$	ANN output prediction
Y_{target}	ANN target training value
ΔP_{bed}	Fluidized bed pressure drop

1. Introduction

Today, society highly depends on fossil fuels such as petroleum and derivates, mineral coal, and natural gas, with 76% of the global primary energy consumed coming from these sources [1]. Thanks to their high energy density, fossil fuels have been a powerful driver of social transformation and technological development of the last century, and the continued increase in global energy demand [2]. However, extensive use of these fuels has led the world to an unprecedented increase in environmental problems such as global warming [3], [4], and health-related issues derived from pollution and toxicity [5].

Researchers have proposed many renewable energy systems to solve this situation [6], [7]. Included are the Hybrid Renewable Energy Systems (HRES) as Microgrids (MG), integrating wind and solar technologies [8]–[10]. Since MG are complex and nonlinear systems, metaheuristic algorithms are an alternative to solve optimal sizing [11] and to improve power generation and energy demand-supply. Bio-inspired optimization algorithms play an important role in the power exchange problem between MG and utility grid, leading to an increment of the power system resilience. In [12], an Energy Management System (EMS) presents a combination of Fuzzy Inference System (FIS) with Genetic Algorithm (GA) to maximize the profit of power exchange; in [13] power exchange problem studied in a multi MG environment combining a game theory Stackelberg game with a Quasi-oppositional Symbiotic Organism Search Algorithm to improve power exchange.

An essential part of an MG is the Energy Storage Systems (ESS), which could be a battery bank or and Energy Backup Power Generation Systems (EBPGS) fed by fossil fuels to provide power when renewable sources are not available. An efficient alternative to fossil fuels for energy backup systems is biomass-derived fuels to supply power in MG [14].

Biomass is neglected despite being a widespread abundant and a Renewable Energy Source (RES) [15]. Some biomass research is focused on finding biomass-derived gas fuels, as Syngas, for power generation applications [16] combined with other RES in MG systems applications [17], [18]. Typical compounds of Syngas are carbon monoxide (CO), hydrogen (H_2) and Methane (CH_4) as energy carriers [19], and because of the partial combustion of biomass in the gasifier, it may also contain appreciable amounts of carbon dioxide (CO_2), nitrogen (N_2) and water (H_2O) [15]. Authors in [20] reviewed on how microgrids integrating syngas generation units improve system resilience to natural disasters and other situations. The Department of Mechanical and Aerospace Engineering at the University of Rome [21] developed an innovative integrated microgrid based on urban waste treatment that enables syngas production intended for small towns where the utility grid may fail, and there is enough urban waste to produce the required syngas. In [22], authors present a method to design an HRES in isolated rural communities in Honduras, considering a syngas power generation unit. They found that adding a syngas gasifier increases the dispatchable power rate when needed.

Beyond experimentation with Syngas gasification plants, researchers need to have models that allow them to understand the dynamics of these systems and the variables involved, and make output predictions to variable inputs [23]. However, mathematical modeling of a Syngas gasification plant is a very complicated and time-consuming task, since it comprises multiple thermal processes and many variables that may affect the mathematical model accuracy [24].

Under this context, bio-inspired algorithms, and specifically Artificial Neural Networks (ANNs), are a powerful tool. ANNs had been widely applied to MG for primary control [25], [26], for prediction [27]–[30], for RES forecast [31] and, for creating black-box models of complex dynamic systems [32]. The tracking of the optimal operating point of a solar photovoltaic (PV) source [33] is achieved by modeling with an ANN part of the controller. Wind Turbine Generator (WTG) maximum power point tracking is achieved using an Adaptative Linear Neuron ANN in [34] by modeling the WTG stator's speed controller. In [35], the authors present a NN model approximation of a DC-DC buck-boost converter to interface a lead-acid battery to a DC-bus. As for the application of ANNs to biomass systems in MG, few works talk about BGP and syngas for power generation. Authors in [36] present a model of a 200 kW_{th} using a dynamic ANN; the presented model estimates the overall behavior of the biomass gasification process and can estimate output variables bases on new measured data with a maximum 15% estimation error. A Multilayer-Perceptron (MLP) and a Radial Basis Function (RBF) ANNs were used and compared to model hydrogen-rich syngas produced from methane dry [37]; results showed that the MLP-based ANN had a better performance in predicting H_2 yield, CO yield, and CH_4 and CO_2 conversions. In [38], authors revealed Syngas for power generation using a Hybrid Thermoelectric Generator (TEG),, a Back Propagation (BP) ANN is used to estimate the open-circuit voltage and maximum power output at the hot-side of the TEG. ANN model is applied to investigate the production of methanol from syngas [39]. A two-inputs seven-hidden layer one-output BP ANN is used in [28] to predict Syngas composition product of palm oil waste gasification showing a suitable approach between experimental and predicted values. In [40], the authors proposed a model for the Prediction of pyrolysis products using eight inputs, one hidden layer, and three outputs ANN. As shown in the literature review, ANNs are applied in various MG, but few in biomass for power generation, with most of the research, focused on the characterization of Syngas or the process itself. We have found no work-related to the coverage of energy demand using syngas and its related biomass gasification process.

This paper aims to provide a reliable ANN-based model of a Biomass Gasification Plant (BGP) for covering the energy demand in an MG using syngas. To accomplish this, a cascade hybrid Feed Forward PSO (FF-PSO) ANN-based model is proposed for predicting syngas and biomass required for a specific energy demand curve. An in-depth analysis of the proposed model compared to a Feed-Forward Back Propagation (FF-BP) ANN and a Cascade-Forward Propagation (CF-P) ANN algorithm is carried out. The validation of the results uses the BGP experimental data at the Renewable Energies Laboratory at the Universitat Politènica de València (LabDER-UPV), Spain.

The organization of this paper is as follows. Section 2 deals with the method, explaining the experimental setup, the presentation of the proposed ANN model, and the training scenarios; Section 3 shows the simulation and experimental results and validation; and, finally, Section 4 summarizes the conclusions of the presented work.

2. Methodology

The methodology followed to create and validate the proposed ANN-based model for the BGP system comprised experimental data gathering, modeling, simulation, and validation. The overall methodology is divided into three crucial stages, as Figure 1 shows.

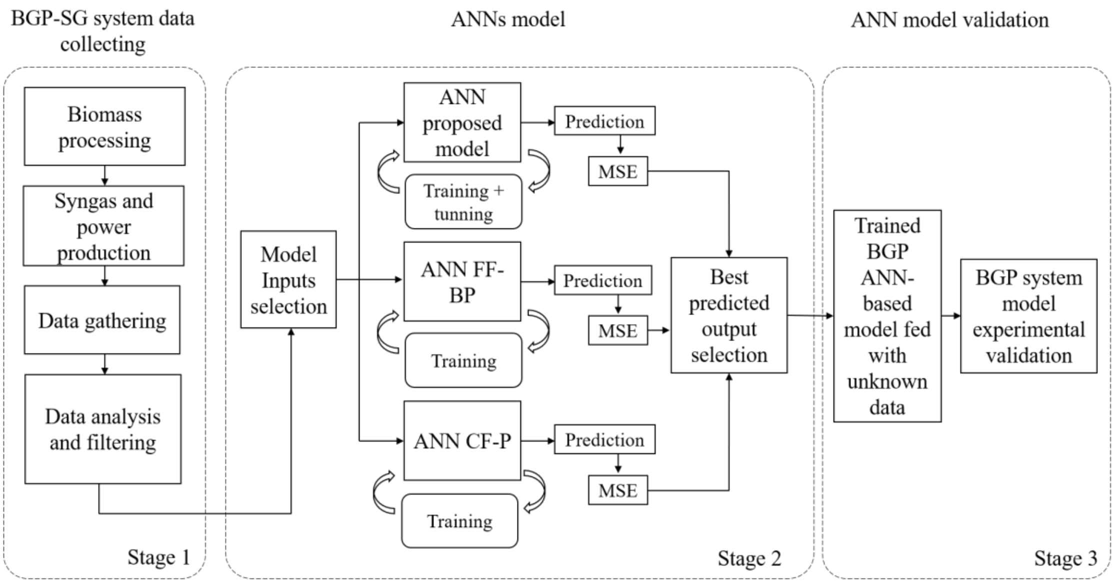

Figure 1 Overall methodology stages for the ANN model design and validation.

As depicted in Figure 1, Stage 1 runs the BGP using empirical input parameters to meet a specific energy demand curve; then, data collection is performed, filtered, and analyzed to select an adequate input parameter for the ANN model.

In Stage 2, three ANN models are trained using input parameters from Stage 1. The proposed ANN-based model is designed to combine a PSO algorithm with a Feed-Forward (FF) ANN to find optimum ANN weights during its training, reducing the Mean Squared Error (MSE) between predicted and real experimentation data. The second model is an FF-BP ANN model designed using MATLAB NNTool, and the third model is a CF-P ANN model also designed using MATLAB NNTool. The number of simulations required for each model depends on both the system dynamics and performing each algorithm for error reduction based on training criteria and parameters for each ANN. An initial scan for each model is required to determine the best adjustment parameters for training the ANN models. After predicted outputs of the ANN models are obtained and evaluated in terms of MSE, the best model is chosen.

Stage 3 is model validation using non-training data. For this purpose, an energy demand curve is fed to the ANN model; then, the model predicts the syngas, biomass, and airflow required by the generator to meet the energy demand. Validation is carried out using the suggested biomass and airflow into the experimental BGP, allowing a real-time approach for biomass required to produce enough syngas for energy demand covering inside an MG. The tests were conducted on an experimental MG located at Universitat Politècnica de València.

2.1. Biomass gasification plant

The BGP system is located at the Distributed Energy Resources Laboratory of the Universitat Politècnica de València, in Spain. (see Figure 2). The entire system comprises a reactor, a gas cleaning system, a gas cooling system, a vacuum pump, the auxiliary elements and the control system. The plant can process from 5 to 13 kg/h of biomass to produce 10 to 28 Nm^3/h at rated power. The gasification system is composed of a 40 kW_{th} gasifier and a 8-10 kW_e. The flow of syngas goes from. The biomass gasification technology selected is based on the bubbling fluidized bed. Table 1 shows the fundamental characteristics of the BGP. Table 2 shows the major feature of the Genset.

(a) (b)

Figure 2 BGP at the LabDER-UPV (a) front and (b) back view.

Table 1 Main features of the biomass gasification plant.

Description	**Feature**
Biomass gasification type	Bubbling fluidized bed
Fuel type	Wood chips (10-15 mm)
	Pellets (6 mm diameter, 15-25 mm length)
Biomass input @ 10%	5 – 13 kg
Biomass flow at power rating	10,5 kg/h
Syngas Low Heating Value (LHV)	5 – 5.8 MJ/m^3
Efficiency at the power rating	70 - 85 %
Syngas production	13 – 33 Nm^3/h

*Adapted from [9], [17], [41]–[43]

Table 2 Main features of the Genset.

Description	**Feature**
Brand	FG Wilson Generator Set
Model	UG14P1
Power rating	10 kW (Natural gas), 8,7 (syngas)
Velocity	1,500 rpm
Compression ratio	8.5:1
Voltage and Frequency	230 V AC, 50Hz

*Adapted from [9], [17], [41]–[43].

Table 3 describes the principal components of the BGP control system. Figure 3 shows the working process of the BGP. The selected inputs for training the ANN, showed in Figure 3, depending on the power generation's performance during the syngas production process from the biomass according to the experimental tests carried out.

Table 3 Main components of the control panel system.

Description	**Device**
Two power meters	Siemens Sentron PAC3200
Power supply @ 240 VAC	Omron CJ1W-PA202
Programmable Logic Device (PLC)	Omron CJ2M-CPU11
Communication module	Omron CJ1W-SCU31
Six-input thermocouple module	Omron CJ1W-TS561
Sixteen digital outputs module	Omron CJ1M-OD212
Variable frequency drive	Omron V1000
HMI touch screen	Omron NS5-SQ10B-V2
Two modules with eight analog inputs	MAC 35080

*Adapted from [9], [43], [44].

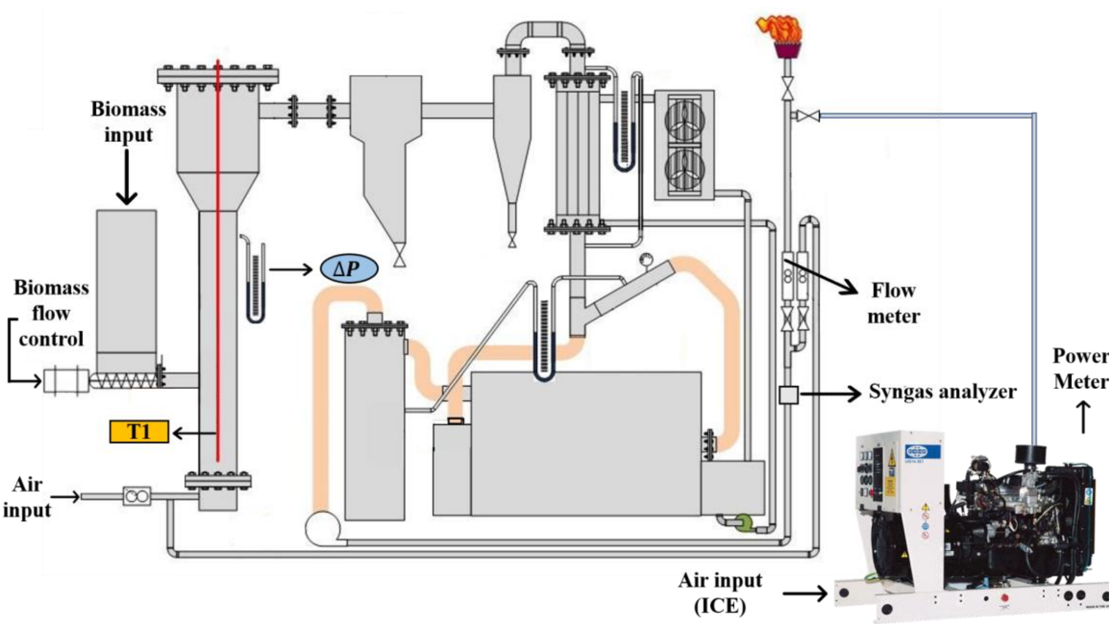

Figure 3 Biomass Gasification Plant and overall diagram.

2.2. Proposed Artificial Neural Network Model

An ANN is a computational bioinspired algorithm based on imitating learning and memorizing a biological brain's capabilities and neural network synapsis. Thanks to the increase of computation power, ANN algorithms are currently an interesting alternative for predictive modeling and control because of their robustness and handling capability for complex nonlinear relationships on dynamic systems.

ANNs must be trained, for this purpose, a set of input training data feeds the Neural Network. The information is processed to get the target data set [45]. When the dispersion between the target data and the real data is small, the ANN is said to be trained and ready to use. An ANN's performance depends on the training procedure and the resulting neuron weights and bias inside its layers [46]. This paper proposes a novel Biogas Gasification (BGP) model using a cascade set of ANNs, each one combined with a PSO algorithm to find optimal neuron weights for each ANN of the model. Figure 4 indicates the input and output of every ANN, in the cascade set of ANN-based model for the BGP.

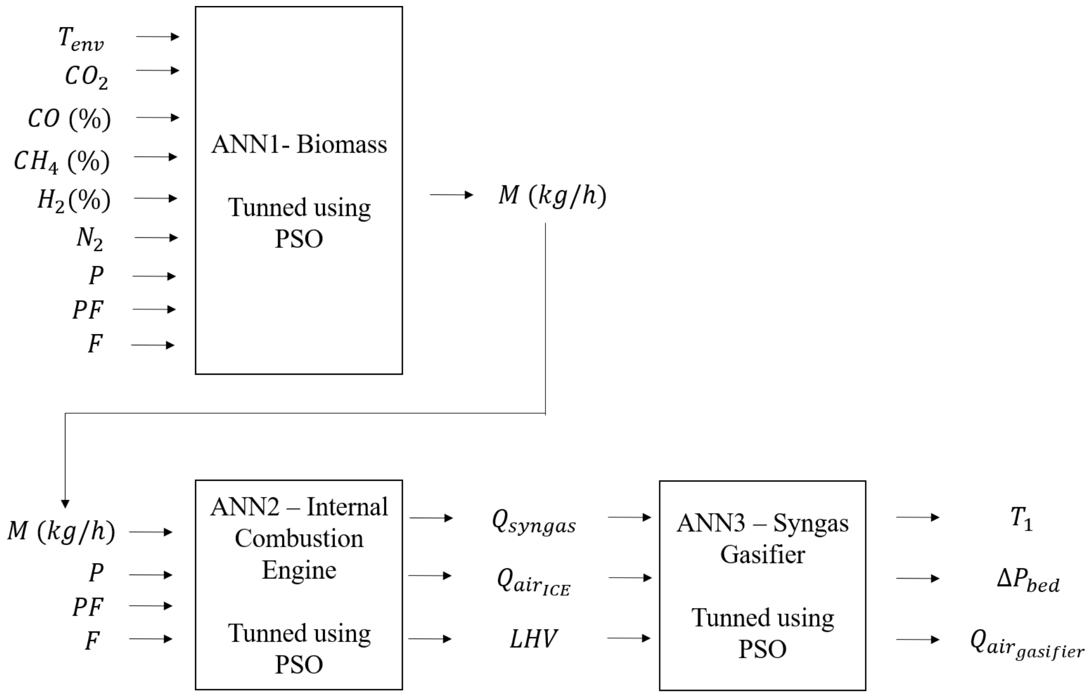

Figure 4 Proposed cascade ANNs PSO tunned model for the BGP.

The proposed ANN-based architecture allows the model to be flexible enough to know just one set of predicted values and intermediate values related to BGP subsystems. The proposed ANN training algorithm uses the PSO algorithm to find optimal neuron weights values, so the MSE between the target and predicted data is minimized. PSO is a bio-inspired optimization algorithm based on animal species' collective intelligence to search, find, and exploit resources [47]. Since neuron weight adjusts during ANN training is a combinatorial problem, PSO can be integrated. Figure 5 illustrates the integration of PSO to an FF ANN.

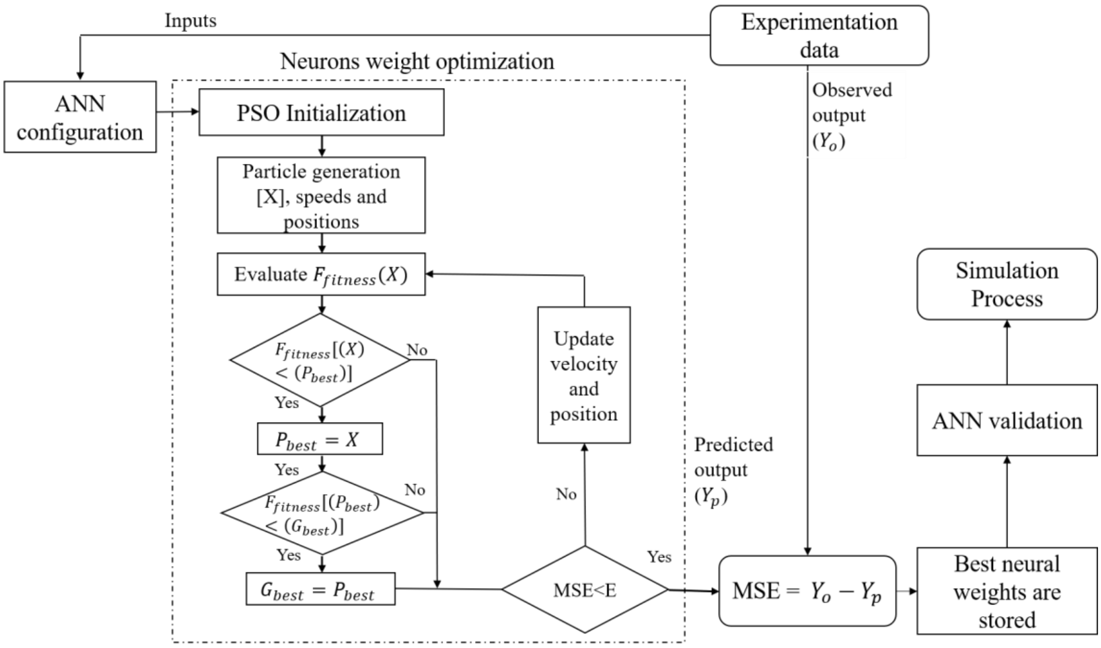

Figure 5 PSO Feed-Forward ANN hybridized model

The input layer of each ANN of the cascade model comprises one neuron for each variable at the input layer. Once the ANN is configured, the PSO is initialized with a random particle population, and then the optimization begins. Optimization variables are ANN weights, represented by the PSO particles, then the performance of the configuration is evaluated using the fitness function whose objective function is to minimize MSE between target and predicted values of the ANN, MSE minimizing is set to an Error (E) stop criteria for the optimization algorithm, the value of this stop criteria depend on the nature of the training and target values of the ANN. The proposed FF ANN is suitable for complex dynamic system modeling and prediction. Layer inside ANN are interconnected via links, and the strength of this link between neuron i and j is defined as weight $w(i, j)$, that must be optimized by the PSO during training. The weighted sum of propagation functions (1-3), determined by inputs in the neurons, is transformed into an activation function (4-6) for the next layer. In that sense, the propagation function of the ANN can be modeled as:

$$ANN_1 = F_{pro_1}\left(o_{i_1}, o_{i_2}, \dots, o_{i_n}, w_{i_1,j}, w_{i_2,j}, \dots, w_{i_n,j}\right) \quad (1)$$

$$ANN_2 = F_{pro_2}\left(o_{i_1}, o_{i_2}, \dots, o_{i_n}, w_{i_1,j}, w_{i_2,j}, \dots, w_{i_n,j}\right) \quad (2)$$

$$ANN_3 = F_{pro_3}\left(o_{i_1}, o_{i_2}, \dots, o_{i_n}, w_{i_1,j}, w_{i_2,j}, \dots, w_{i_n,j}\right) \quad (3)$$

Where $(o_{i_1}, o_{i_2}, \dots, o_{i_n})$ are the weighted output values of the related propagation function F_{pro_n}. The activation function of the ANN is defined by:

$$A_1(t) = F_{act_1}(ANN_1(t), A_1(t-1), \Phi_1\ ) \quad (4)$$

$$A_2(t) = F_{act_2}(ANN_2(t), A_2(t-1), \Phi_2\ ) \quad (5)$$

$$A_3(t) = F_{act_3}(ANN_3(t), A_3(t-1), \Phi_3\ ) \quad (6)$$

Where F_{act_n} is the activation function for each ANN of the proposed model, the network input is $ANN_1(t)$ and the previous activation status is $A_1(t-1)$. The dispersion between target and predicted data depends on the assigned neuron weights inside de ANN. For this purpose, the PSO algorithm is integrated into the proposed model.

Each of the particles of the PSO algorithm represents a neuron weight inside the ANN; these particles have their position, velocity, and acceleration during the search of the optimal solution, the best ANN weights combination so MSE between target and predicted values measured in terms of the MSE. Optimization variables are defined by the vector X_i in (7).

$$X_i = \left[w_{i_1,j}, w_{i_2,j}, \dots, w_{i_n,j}\right] \quad (7)$$

Where $w_{i_n,j}$ are the ANN weights to be optimized for each ANN, and the objective function (8) of the PSO algorithm is:

$$f_{min} \rightarrow \frac{\sum_{n=0}^{N}\left(o_{target} - o_{predicted}\right)}{N} \tag{8}$$

Where o_{target} is the target output value for the ANN training and $o_{predicted}$ is the predicted output value by the ANN model.

The particle for each variable with the best fitness function of all algorithm iterations is called to be the best global g_{best}, and the best result of fitness function evaluated over each particle is called personal best p_{best}. As algorithm iterations progress position will vary, their velocity will be accelerated, pointing to the best solution (9).

$$v_n = w * v_n + c_1 rand(x) * \left(g_{best,n} - x_n\right) \tag{9}$$

Being v_n the updating of particle speed, w is the inertia factor and c_1 and c_2 are acceleration constants.

2.3. Simulation and Training

All three ANN models were trained with the same data set. The training data set was obtained from experimental measurements on the described BGP. In total, 3,408 records were used for each variable. For an ANN training process, the correct choice of input variables, considering their interrelationship and affectation to the system's output, wanted to be predicted for plant modeling. The details of the ANNs models simulated are presented in Table 4.

Table 4 Parameters used for the ANNs models.

Details	**FF-PSO**	**FF-BP**	**CF-P**

Type of ANN	Feed Forward Neural Network	Feed Forward Neural Network	Cascade Forward Neural Network
Training Algorithm	Particle Swarm Optimization	Back Propagation	Propagation
Particle Population	10 – 1000	-	-
C1	1.5 – 2.5	-	-
C2	1.5 – 2.5	-	-
Function for performance	MSE	MSE	MSE
Number of Input Layer	4 – 9	4 – 9	4 – 9
Number of Hidden Layer	1	1	1
Number of Hidden Neurons	1 – 100	1 – 100	1 – 100
Learning Iterations	1000	1000	1000

As shown in Table 4, each ANN model was simulated and tested under different parameters to find the best configuration for each one of them. The training algorithm for each model aims to reduce the error of prediction, adjusting ANN weight, and bias. The performance of the ANN models is measured by the MSE (10), given as,

$$MSE = \frac{1}{N}\sum_{i=1}^{N}\left(Y_{predicted} - Y_{target}\right)^2 \tag{10}$$

Where $Y_{predicted}$ is the output from the ANN, Y_{target} is the experimental data, and N is the number of samples.

Since this work aims to get a model of a BGP using a cascade architecture of a set of ANNs to cover energy demand in an MG, the ANNs inside the model must be trained considering the energy demand curve from the experimental MG. Figure 6 shows the energy demand profile for input data used for training the three different ANN algorithms (FF-BP ANN, CF-P ANN, and the proposed PSO-FF ANN) for evaluation and subsequent choice of best for use.

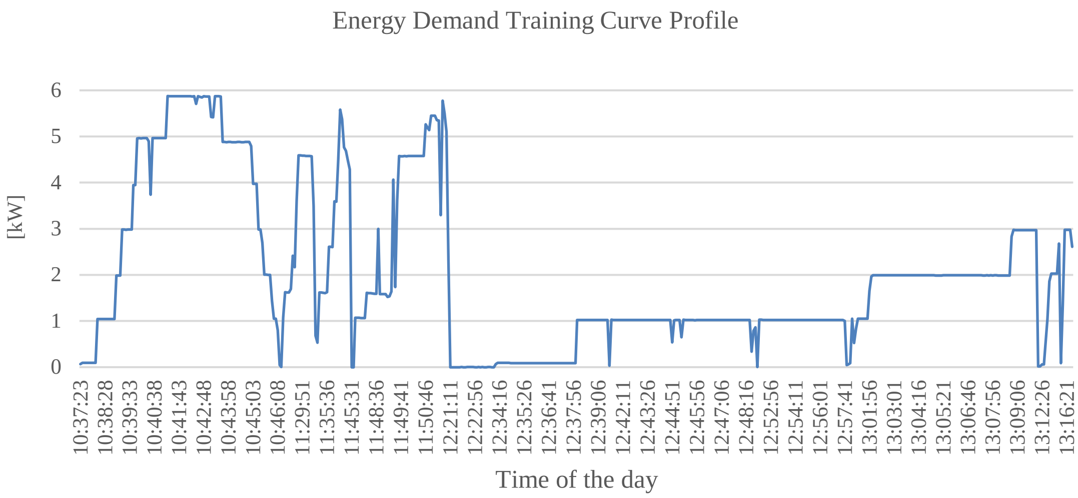

Figure 6 Energy demand curve used for training the cascade ANN-based model of the BGP.

The expected outputs of the model are the best *M* required to produce a Q_{syngas} to be fed into the Internal Combustion Engine (ICE) combined with both airflows of the gasifier and the ICE to generate enough power for energy demand in an AC Microgrid.

3. Results

An ANN-based model for a BGP was developed to estimate biomass required, syngas production, and power generation to cover the energy demand in an AC microgrid. The proposed model comprises a set of three ANNs in a cascade configuration. Prediction of biomass flow (*M*) is carried out for the first ANN inside the model; the second ANN predicts the flow of syngas (Q_{syngas}), the flow of air required by the Genset ($Q_{air_{ICE}}$), and the lower heating value of the syngas (*LHV*); and finally, the temperature inside the reactor (T_1), the bed reactor pressure drop (ΔP_{bed}), and the airflow required by the gasification plant ($Q_{air_{gasifier}}$) are estimated by the third ANN. The proposed model's performance is tested using the MSE for three different training algorithms: FF-PSO, FF-BP, and CF-BP, for each ANN inside the model. With the FF-PSO training algorithm, different values of particle populations, social c_2 and personal c_1 factors were evaluated. 215 simulations were performed to find the optimal ANN configuration of each training algorithm compared in this work. The comparison between the best ANN of each training algorithm is presented in Table 5. For all predicted variables, the lowest MSE values are obtained using the proposed FF-PSO ANN algorithm and the closest to the unitary R-value results.

Table 5 Comparison of MSE and linear regression analysis for best training algorithm results simulated for the ANN-based model.

	FF-PSO		**FF-BP**		**CF-P**	
	MSE	R	MSE	R	MSE	R
$M\ (kg/h)$	0.8198	0.8278	0.9258	0.8105	0.9277	0.8219
Q_{syngas}	0.3464	0.9865	0.5463	0.9710	0.5466	0.9798
$Q_{air_{ICE}}$	45.1225	0.6503	50.6902	0.6430	50.9046	0.6426
LHV	26705	0.7280	29439	0.6757	29491	0.7124
T_1	342.5776	0.6417	497.3452	0.5595	497.1061	0.5536
ΔP_{bed}	1.5659	0.7728	1.9691	0.7210	1.9789	0.7240
$Q_{air_{gasifier}}$	0.4495	0.9531	0.6442	0.9504	0.6451	0.9367

An exploration of various setting up parameters for each ANN training algorithm was done. The number of neurons inside the hidden layer was varied in values from 3, 10, and 100 for the FF-PSO, FF-BP, and CF-P ANNs training algorithms. For the FF-PSO ANN algorithm, besides the number of neurons, it was also tested under different PSO algorithm configurations varying particle population with values of three to four times the dimension of the problem as suggested in other works about PSO algorithm performance using small populations [48]–[50]. However, little attention has been paid to optimal PSO configuration for real-world problems [51], and therefore, for biomass-related problems. An exploration of the PSO performance as an ANN training algorithm is carried out using particle populations of 10, 100, 600, and 1000. The best FF-PSO ANN results were obtained for coefficients c_1 and c_2 values of 1.5 and 2.5 respectively being consistent with other authors findings in different fields of PSO applications [49]. The Table 6 presents a summary of the configurations with best performance for each ANN training algorithm tested.

Table 6 Best ANN training algorithm configurations.

	MSE	**R**	**Input Neurons**	**Hidden Layer Neurons**	**Population (only for PSO)**
FF-PSO					
$M\ (kg/h)$	0.8198	0.8278	9	3	600
Q_{syngas}	0.3464	0.9865	4	3	100
$Q_{air_{ICE}}$	45.1225	0.6503	4	10	1,000
LHV	26705	0.7280	4	10	1,000
T_1	342.5776	0.6417	3	10	600
ΔP_{bed}	1.5659	0.7728	3	10	600
$Q_{air_{gasifier}}$	0.4495	0.9531	3	3	1,000
FF-BP					
$M\ (kg/h)$	0.9258	0.8105	9	100	-
Q_{syngas}	0.5463	0.9800	4	100	-
$Q_{air_{ICE}}$	50.6902	0.6430	4	100	-
LHV	29439	0.6757	4	100	-
T_1	497.3452	0.5595	3	10	-
ΔP_{bed}	1.9691	0.7210	3	3	-
$Q_{air_{gasifier}}$	0.6442	0.9504	3	10	-
CF-P					
$M\ (kg/h)$	0.9277	0.8219	9	100	-
Q_{syngas}	0.5466	0.9797	4	10	-
$Q_{air_{ICE}}$	50.9046	0.6426	4	100	-
LHV	29491	0.7124	4	100	-
T_1	497.0100	0.5536	3	3	-
ΔP_{bed}	1.9789	0.7240	3	100	-

$Q_{air_{gasifier}}$	0.6451	0.9367	3	100	-

As observed in Table 6, the best FF-PSO algorithm performances are obtained for the particle population between 600 and 1000 and three to ten hidden layer neurons; while both for the FF-BP and CF-P best results are achieved for 100 hidden layer neurons in most of the cases, but always with a more significant MSE value compared to the proposed FF-PSO training algorithm. The *R* value evolution for different ANNs configurations training tests and the best *R* plot for biomass flow, syngas flow, ICE inlet airflow, *LHV*, gasifier temperature, fluidized bed pressure drop, and gasifier airflow are shown from Figure 7 to Figure 13.

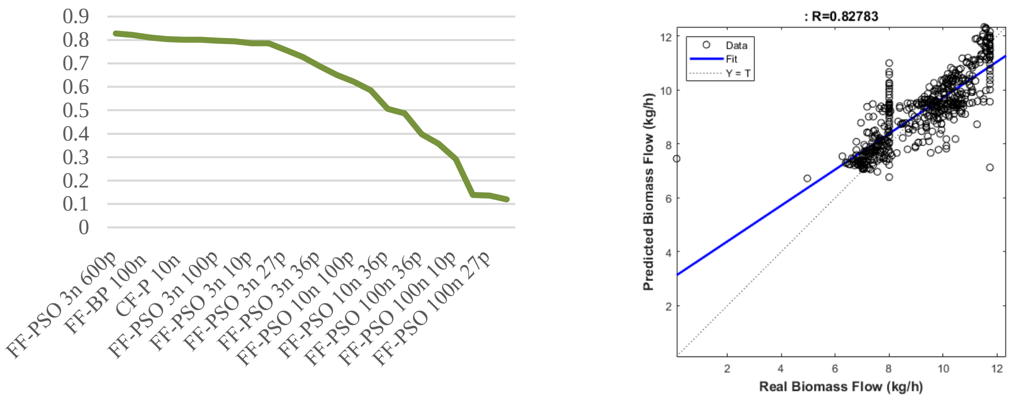

(a) (b)

Figure 7 (a) Linear regression *R* value evolution of Biomass flow for best ANN training algorithm results and (b) best ANN linear regression plot.

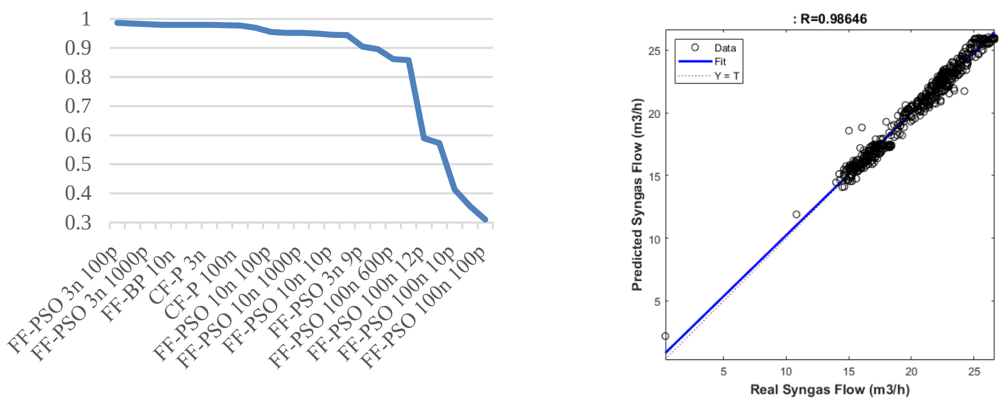

(a) (b)

Figure 8 (a) Linear regression *R* value of Syngas flow for best ANN training algorithm results and (b) best ANN linear regression plot.

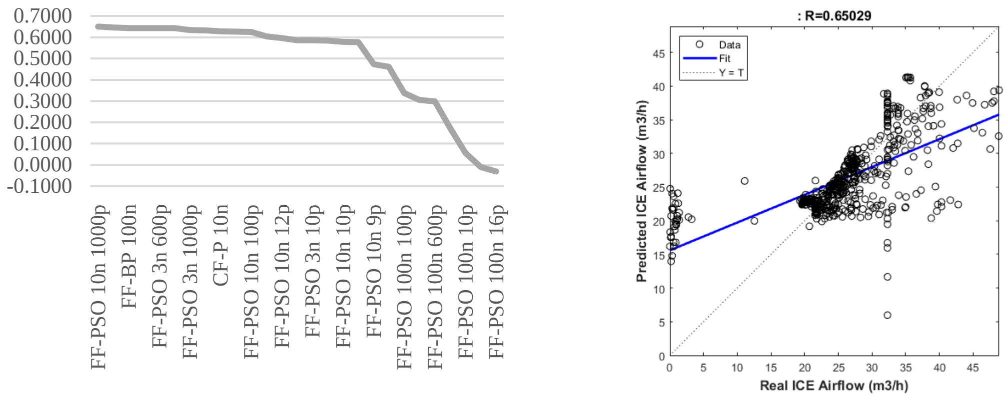

(a) (b)

Figure 9 (a) Linear regression *R* value evolution of ICE inlet airflow for best ANN training algorithm results and (b) best ANN linear regression plot.

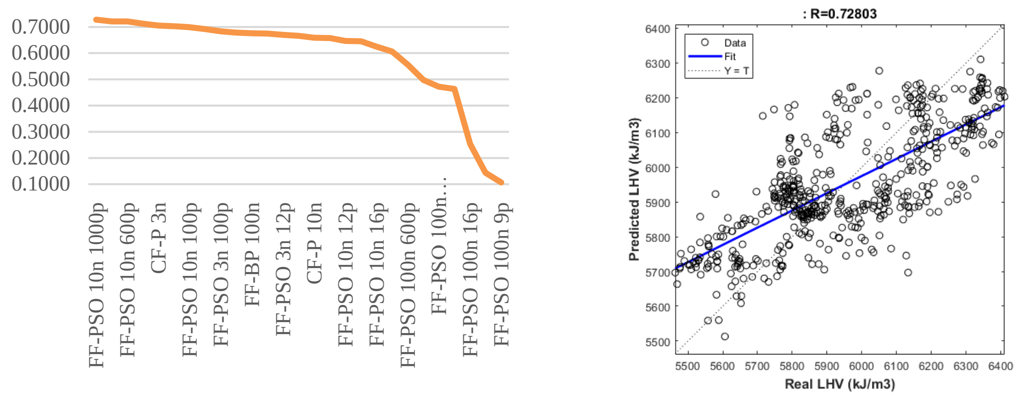

(a) (b)

Figure 10 (a) Linear regression *R* value evolution of LHV for best ANN training algorithm results and (b) best ANN linear regression plot.

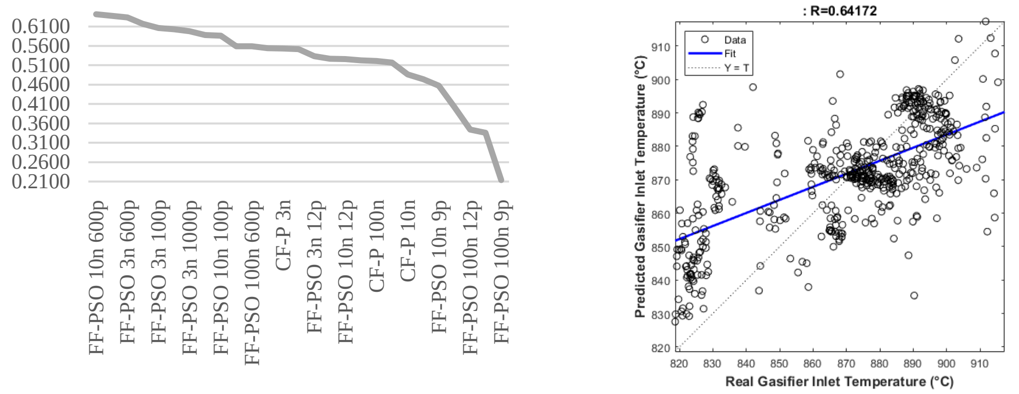

(a) (b)

Figure 11 (a) Linear regression *R* value evolution of Gasifier Inlet Temperature for best ANN training algorithm results and (b) best ANN linear regression plot.

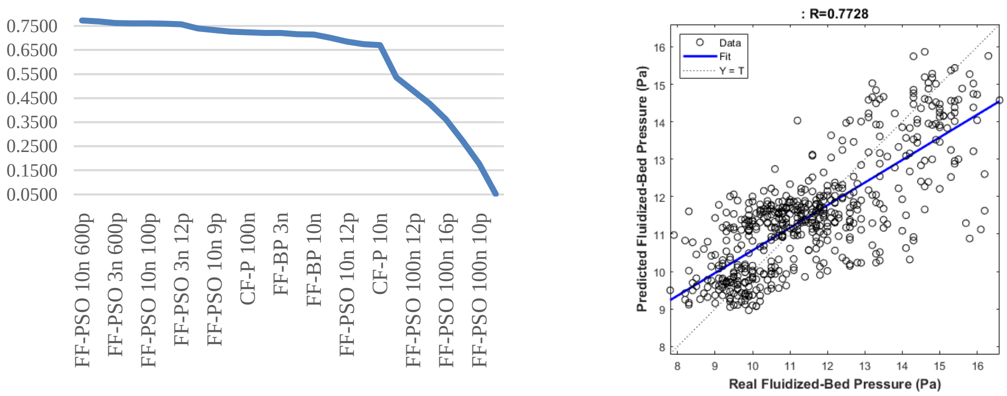

(a) (b)

Figure 12 (a) Linear regression *R* value evolution of Fluidized-Bed Pressure for best ANN training algorithm results and (b) best ANN linear regression plot.

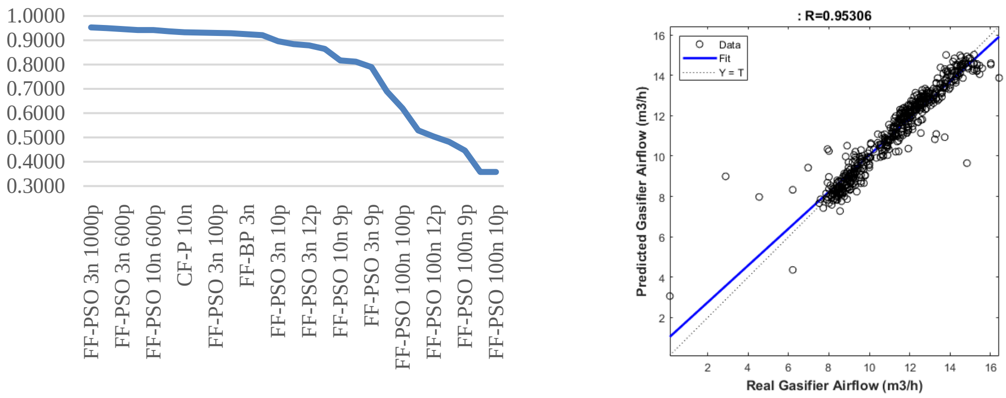

(a) (b)

Figure 13 (a) Linear regression R value evolution of Gasifier airflow for best ANN training algorithm results and (b) best ANN linear regression plot.

High rates of dispersion on linear regression observed in variables (Figure 9 to Figure 12) are caused because of different variable scales used during the process for the individual analysis. The best predictions for each of the variables analyzed are summarized in Table 7.

Table 7 Best predictions for the variables analyzed using the FF-PSO model

	Best MSE, FF-PSO	MSE improvement (FF-PSO respect to FF-BP)	MSE improvement (FF-PSO respect to CF-P)
$M\ (kg/h)$	0.8198	11%	12%
Q_{syngas}	0.3465	37%	37%
$Q_{air_{ICE}}$	26705	11%	11%
T_1	342.5776	31%	31%
ΔP_{bed}	1.5659	20%	21%
$Q_{air_{gasifier}}$	0.4495	30%	30%

A comparison between the biomass flow and Syngas flow predicted by the best ANN of each type of training algorithm is shown in Figure 14 and Figure 14, respectively. It can be seen how ANN trained with the proposed FF-PSO algorithm performs better than ANN trained with FF-BP and CF-P.

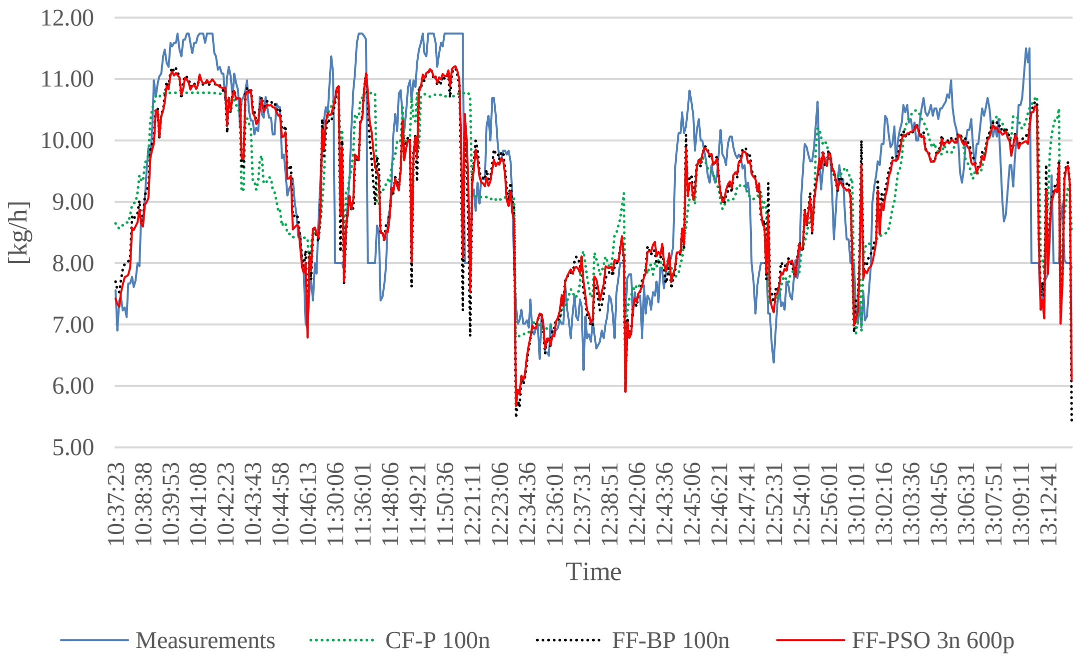

Figure 14 Comparison between best training ANN algorithms and measured data for Biomass flow.

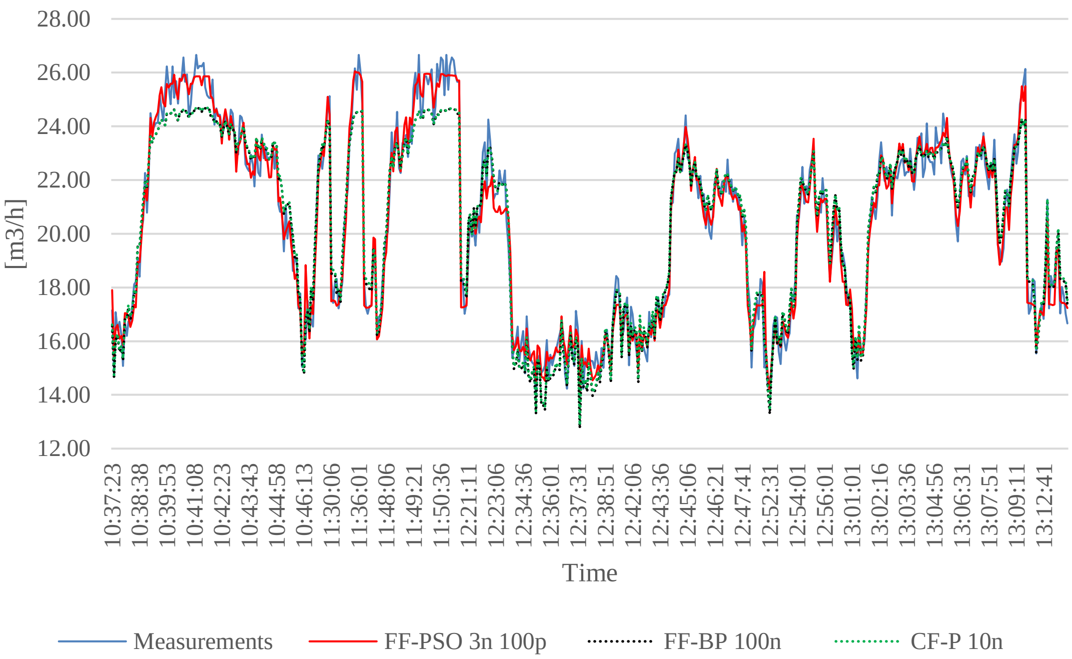

Figure 15 Comparison between best training ANN algorithms and measured data for Syngas flow.

Because of the followed methodology, after tunning and comparing three different training algorithms for the BGP ANN-based model, the ANN-PSO algorithm is chosen, and its best configuration. Figure 16 presents the predicted biomass and syngas' predicted values, using the best algorithm configuration, for the corresponding energy demand curve.

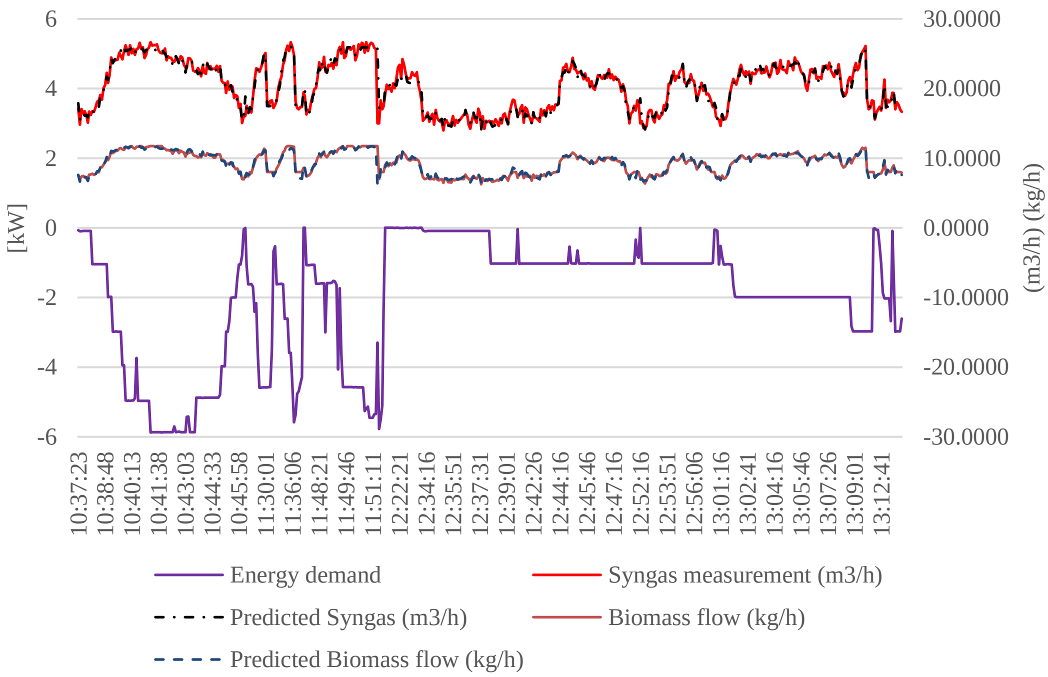

Figure 16 Biomass and Syngas flow required for Energy Demand Covering obtained for the best FF-PSO ANN Training Algorithm.

After the evaluation of the three ANN-based models for the BGP system, the ANN-PSO algorithm was selected as the best training algorithm for this application. The ANN-PSO algorithm got the lowest MSE values (See Figure 16). The results obtained employing the ANN-based model through the proposed FF-PSO were also satisfactory.

The ANN-PSO model was validated to predict biomass and syngas flows required to cover energy demand from an experimental MG. Figure 17 presents the power generation plots, and consumption obtained during experimentation.

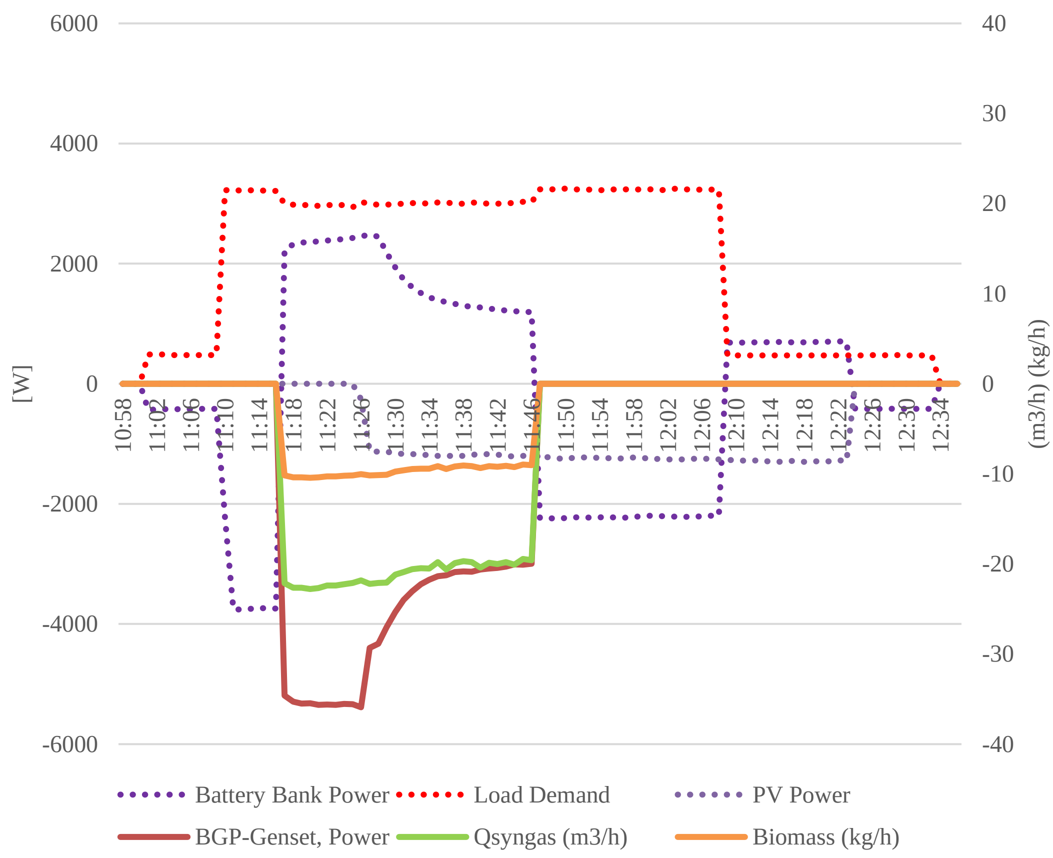

Figure 17 Energy Demand, required biomass, and produced Syngas and Power Plots of MG Experimentation Scenario.

The power produced by the BGP can be predicted and decomposed in the required biomass flow and the produced syngas flow used to feed the ICE (Figure 17). The ANN-based model proposed by this methodology allows a real-time estimation of both the syngas required by the ICE and the biomass required for the BGP to cover the energy demand of the MG.

4. Conclusions

In this article, a novel ANN-based model applied to a BGP system has been presented and validated. Since ANNs inside the model need to be trained, three different ANN training algorithms were evaluated: FF-PSO, FF-BP, and CF-P. Training algorithms performance has been measured using MSE, under different ANN configurations: varying number of hidden layers neurons; and different PSO configuration parameters for the FF-PSO, varying population size from 9 to 1000, and $c_1$and c_2 coefficients were varied from 1.5 to 2.5 values.

An experimental MG provided the energy demand curve to be supplied into the proposed ANN-based model to predict, as the main model outputs, the required biomass flow, and syngas flow to cover the energy demand. The cascade architecture of the model also allows the prediction of the airflow required by the ICE, the LHV, the temperature, the pressure drop in the bed, and the airflow required for the gasification process. The results showed that the FF-PSO proposed for the ANN-based model has the best performance, obtaining, on average for all variables analyzed, an MSE of 23.3% lower compared to the FF-BP and CF-P models. Also, better linear regressions values were obtained. The reached ANN-based model can be applied in a real-time approach to control and manage the BGP.

As a general conclusion, the presented ANN-model applied to a BGP and the proposed FF-PSO algorithm showed to solve model dynamic Power Generation systems. The PSO is an efficient algorithm to train the ANN. The best results were obtained for a few hidden layer neurons (1 to 3), a high number of particle populations (600 to 1000), and standard c_1 and c_2 coefficients (1.5 to 2.5).

In future work is planned to extend the ANN-model to other MG subsystems, allowing effective control for the energy management of the MG.

5. Acknowledgments

The authors would like to thank Consejo Nacional de Ciencia y Tecnología (CONACYT) for their support of funding this work under the 487628 and 486670 scholarship numbers. The authors express their sincere appreciation to Universitat Politènica de València for

the facilities to perform the tests for the proposed algorithm at the Renewable Energies Laboratory (LabDER) of the Institute for Energy Engineering.

6. References

[1] S. Ramalingam, M. Ezhumalai, and M. Govindasamy, "Syngas: Derived from biodiesel and its influence on CI engine," *Energy*, 2019, doi: 10.1016/j.energy.2019.116189.

[2] D. Mallick, P. Mahanta, and V. S. Moholkar, "Co-gasification of coal and biomass blends: Chemistry and engineering," *Fuel*, vol. 204. Elsevier Ltd, pp. 106–128, Sep. 2017, doi: 10.1016/j.fuel.2017.05.006.

[3] I. Hanif, S. M. Faraz Raza, P. Gago-de-Santos, and Q. Abbas, "Fossil fuels, foreign direct investment, and economic growth have triggered CO2 emissions in emerging Asian economies: Some empirical evidence," *Energy*, vol. 171, pp. 493–501, Mar. 2019, doi: 10.1016/j.energy.2019.01.011.

[4] F. Martins, C. Felgueiras, M. Smitkova, and N. Caetano, "Analysis of Fossil Fuel Energy Consumption and Environmental Impacts in European Countries," *Energies*, vol. 12, no. 6, p. 964, Mar. 2019, doi: 10.3390/en12060964.

[5] C. Gaete-Morales, A. Gallego-Schmid, L. Stamford, and A. Azapagic, "Life cycle environmental impacts of electricity from fossil fuels in Chile over a ten-year period," *J. Clean. Prod.*, vol. 232, pp. 1499–1512, Sep. 2019, doi: 10.1016/j.jclepro.2019.05.374.

[6] P. Carneiro *et al.*, "Electromagnetic energy harvesting using magnetic levitation architectures: A review," *Appl. Energy*, vol. 260, no. July 2019, p. 114191, 2020, doi: 10.1016/j.apenergy.2019.114191.

[7] V. Slabov, S. Kopyl, M. P. Soares dos Santos, and A. L. Kholkin, "Natural and Eco-Friendly Materials for Triboelectric Energy Harvesting," *Nano-Micro Lett.*,

vol. 12, no. 1, pp. 1–18, 2020, doi: 10.1007/s40820-020-0373-y.

[8] M. S. S. Danish, H. Matayoshi, H. R. Howlader, S. Chakraborty, P. Mandal, and T. Senjyu, “Microgrid Planning and Design: Resilience to Sustainability,” in *2019 IEEE PES GTD Grand International Conference and Exposition Asia, GTD Asia 2019*, May 2019, pp. 253–258, doi: 10.1109/GTDAsia.2019.8716010.

[9] A. Pérez-Navarro *et al.*, “Experimental verification of hybrid renewable systems as feasible energy sources,” *Renew. Energy*, vol. 86, pp. 384–391, 2016, doi: 10.1016/j.renene.2015.08.030.

[10] E. Hurtado, E. Peñalvo-López, A. Pérez-Navarro, C. Vargas, and D. Alfonso, “Optimization of a hybrid renewable system for high feasibility application in non-connected zones,” *Appl. Energy*, vol. 155, 2015, doi: 10.1016/j.apenergy.2015.05.097.

[11] A. L. Bukar, C. W. Tan, and K. Y. Lau, “Optimal sizing of an autonomous photovoltaic/wind/battery/diesel generator microgrid using grasshopper optimization algorithm,” *Sol. Energy*, vol. 188, pp. 685–696, Aug. 2019, doi: 10.1016/j.solener.2019.06.050.

[12] S. Leonori, M. Paschero, F. M. Frattale Mascioli, and A. Rizzi, “Optimization strategies for Microgrid energy management systems by Genetic Algorithms,” *Appl. Soft Comput. J.*, vol. 86, p. 105903, Jan. 2020, doi: 10.1016/j.asoc.2019.105903.

[13] J. Aguila-Leon, C. Chiñas-Palacios, E. X. M. Garcia, and C. Vargas-Salgado, “A multimicrogrid energy management model implementing an evolutionary game-theoretic approach,” *Int. Trans. Electr. Energy Syst.*, vol. n/a, no. n/a, p. e12617, Sep. 2020, doi: 10.1002/2050-7038.12617.

[14] Danish and Z. Wang, “Does biomass energy consumption help to control

environmental pollution? Evidence from BRICS countries," *Sci. Total Environ.*, vol. 670, pp. 1075–1083, Jun. 2019, doi: 10.1016/j.scitotenv.2019.03.268.

[15] H. W. Gitano-Briggs and K. L. Kean, "Genset Optimization for Biomass Syngas Operation," *Renew. Energy - Util. Syst. Integr.*, 2016, doi: 10.5772/62727.

[16] C. Rodríguez-Monroy, G. Mármol-Acitores, and G. Nilsson-Cifuentes, "Electricity generation in Chile using non-conventional renewable energy sources – A focus on biomass," *Renewable and Sustainable Energy Reviews*, vol. 81. Elsevier Ltd, pp. 937–945, Jan. 2018, doi: 10.1016/j.rser.2017.08.059.

[17] C. Y. Acevedo-Arenas *et al.*, "MPC for optimal dispatch of an AC-linked hybrid PV/wind/biomass/H2 system incorporating demand response," *Energy Convers. Manag.*, vol. 186, pp. 241–257, Apr. 2019, doi: 10.1016/j.enconman.2019.02.044.

[18] M. S. Aziz, M. A. Khan, A. Khan, F. Nawaz, M. Imran, and A. Siddique, "Rural Electrification through an Optimized Off-grid Microgrid based on Biogas, Solar, and Hydro Power," Feb. 2020, doi: 10.1109/ICEET48479.2020.9048222.

[19] X. Kan, D. Zhou, W. Yang, X. Zhai, and C. H. Wang, "An investigation on utilization of biogas and syngas produced from biomass waste in premixed spark ignition engine," *Appl. Energy*, vol. 212, pp. 210–222, Feb. 2018, doi: 10.1016/j.apenergy.2017.12.037.

[20] A. A. Bajwa, H. Mokhlis, S. Mekhilef, and M. Mubin, "Enhancing power system resilience leveraging microgrids: A review," *Journal of Renewable and Sustainable Energy*, vol. 11, no. 3. American Institute of Physics Inc., p. 35503, May 2019, doi: 10.1063/1.5066264.

[21] L. Cedola and A. Tallini, "Development of an Innovative Microgrid: 2MSG−Micro Mobile Smart Grid."

[22] D. Ribó-Pérez, P. Bastida-Molina, T. Gómez-Navarro, and E. Hurtado-Pérez, "Hybrid assessment for a hybrid microgrid: A novel methodology to critically analyse generation technologies for hybrid microgrids," *Renew. Energy*, vol. 157, pp. 874–887, Sep. 2020, doi: 10.1016/j.renene.2020.05.095.

[23] N. Cerone, F. Zimbardi, L. Contuzzi, J. Baleta, D. Cerinski, and R. Skvorčinskienė, "Experimental investigation of syngas composition variation along updraft fixed bed gasifier," *Energy Convers. Manag.*, vol. 221, p. 113116, Oct. 2020, doi: 10.1016/j.enconman.2020.113116.

[24] J. Ren, J. P. Cao, X. Y. Zhao, F. L. Yang, and X. Y. Wei, "Recent advances in syngas production from biomass catalytic gasification: A critical review on reactors, catalysts, catalytic mechanisms and mathematical models," *Renewable and Sustainable Energy Reviews*, vol. 116. Elsevier Ltd, p. 109426, Dec. 2019, doi: 10.1016/j.rser.2019.109426.

[25] T. C. Ou and C. M. Hong, "Dynamic operation and control of microgrid hybrid power systems," *Energy*, vol. 66, pp. 314–323, Mar. 2014, doi: 10.1016/j.energy.2014.01.042.

[26] V. Sandeep, V. Bala Murali Krishna, K. K. Namala, and D. N. Rao, "Grid connected wind power system driven by PMSG with MPPT technique using neural network compensator," in *2016 International Conference on Energy Efficient Technologies for Sustainability, ICEETS 2016*, Oct. 2016, pp. 917–921, doi: 10.1109/ICEETS.2016.7583879.

[27] W. A. Alsulami and R. Sreerama Kumar, "Artificial neural network based load flow solution of Saudi national grid," in *2017 Saudi Arabia Smart Grid Conference, SASG 2017*, May 2018, pp. 1–7, doi: 10.1109/SASG.2017.8356516.

[28] M. Shahbaz *et al.*, "Artificial neural network approach for the steam gasification

of palm oil waste using bottom ash and CaO," *Renew. Energy*, vol. 132, pp. 243–254, 2019, doi: 10.1016/j.renene.2018.07.142.

[29] M. Taghavi, A. Gharehghani, F. B. Nejad, and M. Mirsalim, "Developing a model to predict the start of combustion in HCCI engine using ANN-GA approach," *Energy Convers. Manag.*, vol. 195, no. April, pp. 57–69, 2019, doi: 10.1016/j.enconman.2019.05.015.

[30] F. Yang, H. Cho, H. Zhang, J. Zhang, and Y. Wu, "Artificial neural network (ANN) based prediction and optimization of an organic Rankine cycle (ORC) for diesel engine waste heat recovery," *Energy Convers. Manag.*, vol. 164, no. February, pp. 15–26, 2018, doi: 10.1016/j.enconman.2018.02.062.

[31] A. Heydari, D. Astiaso Garcia, F. Keynia, F. Bisegna, and L. De Santoli, "A novel composite neural network based method for wind and solar power forecasting in microgrids," *Appl. Energy*, vol. 251, p. 113353, Oct. 2019, doi: 10.1016/j.apenergy.2019.113353.

[32] T. B. Lopez-Garcia, A. Coronado-Mendoza, and J. A. Domínguez-Navarro, "Artificial neural networks in microgrids: A review," *Eng. Appl. Artif. Intell.*, vol. 95, p. 103894, Oct. 2020, doi: 10.1016/j.engappai.2020.103894.

[33] N. Chettibi and A. Mellit, "Intelligent control strategy for a grid connected PV/SOFC/BESS energy generation system," *Energy*, vol. 147, pp. 239–262, Mar. 2018, doi: 10.1016/j.energy.2018.01.030.

[34] N. Chettibi, A. Mellit, G. Sulligoi, and A. Massi Pavan, "Adaptive Neural Network-Based Control of a Hybrid AC/DC Microgrid," *IEEE Trans. Smart Grid*, vol. 9, no. 3, pp. 1667–1679, May 2018, doi: 10.1109/TSG.2016.2597006.

[35] T. B. Lopez-Garcia, R. Ruiz-Cruz, and E. N. Sanchez, "Real-Time Battery Bank Charge-Discharge Using Neural Sliding Mode Control," in *Proceedings of the*

International Joint Conference on Neural Networks, Oct. 2018, vol. 2018-July, doi: 10.1109/IJCNN.2018.8489533.

[36] A. Salah, L. Hanel, M. Beirow, and G. Scheffknecht, *Modelling SER Biomass Gasification Using Dynamic Neural Networks*, vol. 38. Elsevier Masson SAS, 2016.

[37] M. A. Hossain, B. V. Ayodele, C. K. Cheng, and M. R. Khan, “Artificial neural network modeling of hydrogen-rich syngas production from methane dry reforming over novel Ni/CaFe2O4 catalysts,” *Int. J. Hydrogen Energy*, vol. 41, no. 26, pp. 11119–11130, 2016, doi: 10.1016/j.ijhydene.2016.04.034.

[38] A. A. Angeline, J. Jayakumar, L. G. Asirvatham, and S. Wongwises, “Power generation from combusted ‘Syngas’ using hybrid thermoelectric generator and forecasting the performance with ANN technique,” *J. Therm. Eng.*, vol. 4, no. 4, pp. 2149–2168, 2018, doi: 10.18186/journal-of-thermal-engineering.433806.

[39] J. Ye, “Artificial neural network modeling of methanol production from syngas,” *Pet. Sci. Technol.*, vol. 37, no. 6, pp. 629–632, 2019, doi: 10.1080/10916466.2018.1560321.

[40] B. Aydinli, A. Caglar, S. Pekol, and A. Karaci, “The prediction of potential energy and matter production from biomass pyrolysis with artificial neural network,” *Energy Explor. Exploit.*, vol. 35, no. 6, pp. 698–712, 2017, doi: 10.1177/0144598717716282.

[41] D. Alfonso-solar, C. Vargas-Salgado, C. Sánchez-díaz, and E. Hurtado-pérez, “Small-scale hybrid photovoltaic-biomass systems feasibility analysis for higher education buildings,” *Sustain.*, vol. 12, no. 21, pp. 1–11, 2020, doi: 10.3390/su12219300.

[42] C. Vargas-Salgado, E. Hurtado-Pérez, D. Alfonso-Solar, and A. Malmquist,

"Empirical Design , Construction , and Experimental Test of a Small - Scale Bubbling Fluidized Bed Reactor," *Sustain.*, vol. 13, no. 3, pp. 1–23, 2021, [Online]. Available: https://www.mdpi.com/2071-1050/13/3/1061 .

[43] E. Hurtado, E. Peñalvo-López, Á. Pérez-Navarro, C. Vargas, and D. Alfonso, "Optimization of a hybrid renewable system for high feasibility application in non-connected zones," *Appl. Energy*, vol. 155, pp. 308–314, Oct. 2015, doi: 10.1016/J.APENERGY.2015.05.097.

[44] C. Vargas-Salgado, J. Aguila-Leon, C. Chiñas-Palacios, and E. Hurtado-Perez, "Low-cost web-based Supervisory Control and Data Acquisition system for a microgrid testbed: A case study in design and implementation for academic and research applications," *Heliyon*, vol. 5, no. 9, Sep. 2019, doi: 10.1016/j.heliyon.2019.e02474.

[45] W. O. Griffin and J. A. Darsey, "Artificial neural network prediction indicators of density functional theory metal hydride models," *Int. J. Hydrogen Energy*, vol. 38, no. 27, pp. 11920–11929, Sep. 2013, doi: 10.1016/j.ijhydene.2013.06.138.

[46] B. V. Ayodele and C. K. Cheng, "Modelling and optimization of syngas production from methane dry reforming over ceria-supported cobalt catalyst using artificial neural networks and Box-Behnken design," *J. Ind. Eng. Chem.*, vol. 32, pp. 246–258, Dec. 2015, doi: 10.1016/j.jiec.2015.08.021.

[47] J. Aguila-Leon, C. D. Chinas-Palacios, C. Vargas-Salgado, E. Hurtado-Perez, and E. X. M. Garcia, "Optimal PID Parameters Tunning for a DC-DC Boost Converter: A Performance Comparative Using Grey Wolf Optimizer, Particle Swarm Optimization and Genetic Algorithms," Jul. 2020, pp. 1–6, doi: 10.1109/sustech47890.2020.9150507.

[48] F. van den Bergh and A. P. Engelbrecht, "A cooperative approach to participle

swam optimization," *IEEE Trans. Evol. Comput.*, vol. 8, no. 3, pp. 225–239, Jun. 2004, doi: 10.1109/TEVC.2004.826069.

[49] L. P. Zhang, H. J. Yu, and S. X. Hu, "Optimal choice of parameters for particle swarm optimization," *J. Zhejiang Univ. Sci.*, vol. 6 A, no. 6, pp. 528–534, Jun. 2005, doi: 10.1631/jzus.2005.A0528.

[50] M. R. Bonyadi and Z. Michalewicz, "Particle swarm optimization for single objective continuous space problems: A review," *Evolutionary Computation*, vol. 25, no. 1. MIT Press Journals, pp. 1–54, Mar. 2017, doi: 10.1162/EVCO_r_00180.

[51] A. P. Piotrowski, J. J. Napiorkowski, and A. E. Piotrowska, "Population size in Particle Swarm Optimization," *Swarm Evol. Comput.*, vol. 58, p. 100718, Nov. 2020, doi: 10.1016/j.swevo.2020.100718.